RSC Advances

PAPER

View Article Online
View Journal | View Issue

Cite this: *RSC Adv.*, 2022, **12**, 18209

Targeted drug release system based on pH-responsive PAA-POSS nanoparticles†

Won Jung Kim,[a] Eu Hyun Lee,[a] Yong-Jin Kwon,[b] Sang-Kyu Ye*[b] and Kyu oh Kim *[a]

Received 20th February 2022
Accepted 5th May 2022

DOI: 10.1039/d2ra01141g

rsc.li/rsc-advances

An amphipathic PAA-POSS@DOX drug delivery system that responds sensitively to pH changes in the cancer microenvironment has been developed using a nanoparticle based on inorganic polyhedral oligomeric silsesquioxane (POSS). POSS was introduced to the carboxylic acid group of polyacrylic acid to which doxorubicin anticancer drug was loaded to prepare 480 ± 192 nm self-assembled nanoparticles. PAA-POSS had a high loading efficiency of over 75% and doxorubicin was quickly released to the target area responding sensitively to weakly acidic conditions. The possibility of employing PAA-POSS as a targeted drug delivery system has been confirmed by observing the death of cells of the MDA-MB-231 breast cancer line.

Introduction

Amphiphilic polymer nanoparticles, as excellent nanocarriers, have received tremendous attention in research on drug delivery systems (DDSs), especially for chemotherapy drugs, genes and proteins. For instance, amphiphilic polymers constructing the core–shell architecture have been applied in the solubilization of hydrophobic drugs. POSS (polyhedral oligosilsesquioxane) is a spherical inorganic material 1–3 nm in size with a high surface energy and internal pores. As a nanodrug delivery system, POSS has biocompatibility, high drug loading capacity, and physical and biochemical stability but research on it is limited.[1–9] Recently, pH-sensitive targeted drug delivery systems that can deliver anticancer drugs to the target and allow them to react with tumor tissues or cellular endosomes are actively being developed. It is reported that the pH values of tumor sites are much more acidic (*ca.* pH 5.0–6.0) than blood and the intracellular pH of their endosomes and lysosomes.[10–19] To design a drug delivery system that reacts sensitively with the tumor area over the surrounding normal tissues and releases the drug, PAA (polyacrylic acid) was selected as its carboxylic acid proton that can be substituted with POSS molecules around pH 5.0. POSS is attached to the carboxylic acid groups of PAA to prepare the organic/inorganic drug delivery system.[20–23] The carboxyl group dissociates to the COO^- ion depending on the pH and becomes soluble. To prepare a PAA complex that can be rapidly solubilized and solidified by slight changes in the environment, POSS is attached so that the accessibility of the carboxyl group can be increased by the bulky POSS. Its strong hydrophobic character also maximizes the loading capacity and enhances the physical stability of the drug delivery system. Amphiphilic PAA-POSS is prepared without using toxic catalysts or organic solvents and its synthesis is confirmed by FT-IR, ^{1}H-NMR, XPS, TEM, and TGA.[24] PAA-POSS has a higher loading capacity than PAA, and the doxorubicin (DOX)-loaded PAA-POSS@DOX reacts sensitively to pH to quickly release the anticancer drug under acidic conditions. The ability of PAA-POSS@DOX to kill MDA-MB-231 breast cancer cells has been confirmed by *in vitro* experiments.

Results and discussion

We have developed an improved nanocarrier for potential clinical use that addresses several specific issues important to nanocarrier design: process formulation, biocompatibility, specificity, detectability, drug capacity and efficacy. We have synthesized non-toxic PAA 5.0K-POSS macromers for esterification, which can occur between the PAA carboxyl groups and the hydroxyl groups of POSS, and have characterized them. PAA-POSS was synthesized simply by heating in the presence of an acid catalyst, as shown in Scheme 1. One (PAA-POSS(10 : 1)) or five (PAA-POSS(10 : 5)) of the 10 carboxyl groups of PAA were substituted with POSS. Based on an initial study, this study was carried out by selecting PAA-POSS(10 : 1), which is effective in killing MDA-MB-231 cancer cells at Fig. S1.† FT-IR and ^{1}H-NMR analyses were carried out to verify the synthesis of PAA-POSS, as shown in Fig. 1 and 3(c).

The –OH peaks of PAA, POSS, and PAA-POSS@DOX can be seen at 3450 cm^{-1} and 1330∼1470 cm^{-1} (Fig. 1(a)). The presence of ether groups in POSS, and PAA-POSS@DOX is confirmed by the peak at 1232 cm^{-1}. The characteristic Si–O–Si peak of POSS can be seen around 1110 cm^{-1}. The carbonyl peaks of PAA

[a]*Department of Fiber System Engineering, Dankook University, 152, Jookjeon-ro, Suji-gu, Yongin-si, Gyeonggi-do, 448-701, Republic of Korea*

[b]*Department of Pharmacology, Seoul National University College of Medicine, Republic of Korea. E-mail: sangkyu@snu.ac.kr*

† Electronic supplementary information (ESI) available. See https://doi.org/10.1039/d2ra01141g

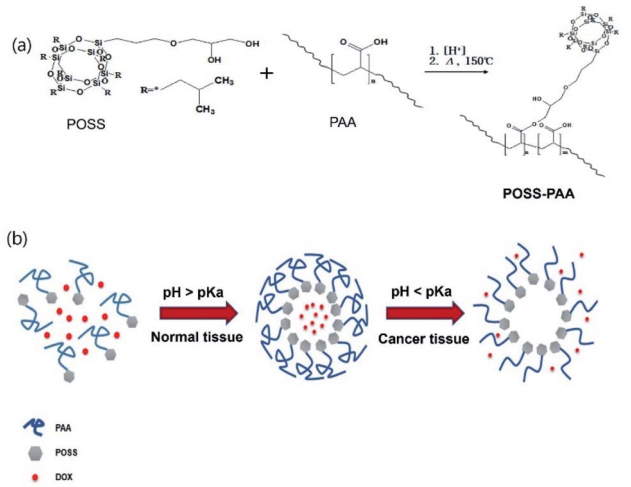

Scheme 1 (a) Synthetic route of POSS-PAA (b) DOX-releasing mechanism of the pH-specific response of PAA-POSS@DOX at acidic pH.

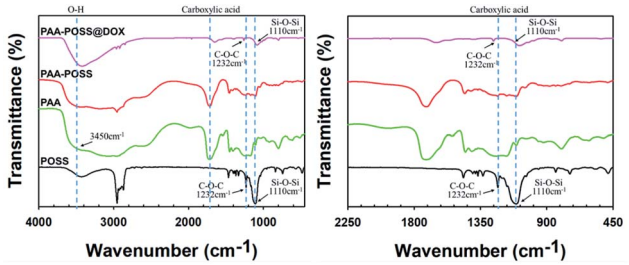

Fig. 1 FT-IR spectra of POSS, PAA, PAA-POSS, and PAA-POSS@DOX at wavenumbers of 4000–400 cm^{-1} (left) and 2250–450 cm^{-1} (right).

carboxylic acid groups and PAA-POSS@DOX ester groups can be seen at 1715 cm^{-1} and 1735 cm^{-1}, respectively. A shift in the peak position of the ester groups occurs with increasing POSS content. The ^{1}H-NMR of PAA-POSS in Fig. 3(d) shows the characteristic peaks of PAA and those of POSS at 1.85 (7H, –Si–$CH_2CH(CH_3)_2$), 1.43 (14H, –Si–$CH_2CH(CH_3)_2$), and 0.95 (42H, –Si–$CH_2CH(CH_3)_2$).

The XPS spectra of PAA and PAA-POSS in Fig. 2 show the element type, composition, and information about the bonding of the carboxylic acid group with POSS. The Si 2s and Si 2p peaks of POSS can be confirmed in the survey XPS. The analysis of C 1s shows a peak at 284.78 eV, characteristic of the sp^3 structure, a peak at 286.40 eV, characteristic of the C–O–C structure, and a peak at 289.3 eV, characteristic of the C=O structure. As POSS reacts with the carboxylic acid groups abundant in PAA, the intensity of the peak due to the carboxylic acid group decreases from 23% to 6% and the overlapping peak at 289 eV due to ester groups increases from 5% to 24%. In the O 1s spectra, intensity of the C–O peak at 533 eV decreases to half of that in PAA-POSS.

TEM analysis was carried out to characterize the shape and size of PAA-POSS@DOX and PAA@DOX, as shown in Fig. 3(a). The average particle sizes of PAA-POSS@DOX and PAA@DOX were 480 ± 192 nm and 630 ± 277 nm, respectively.

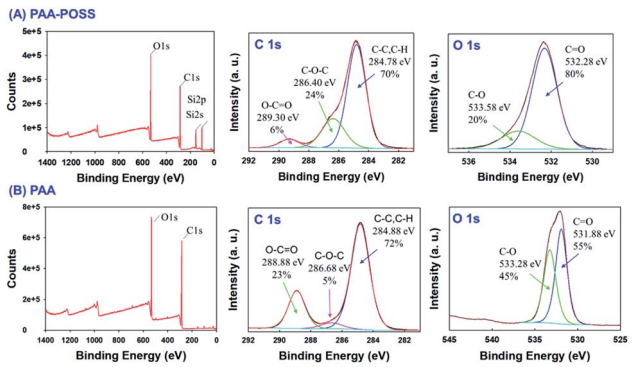

Fig. 2 The survey data and deconvolution of the high-resolution XPS spectra of C 1s and O 1s of (A) PAA-POSS and (B) PAA.

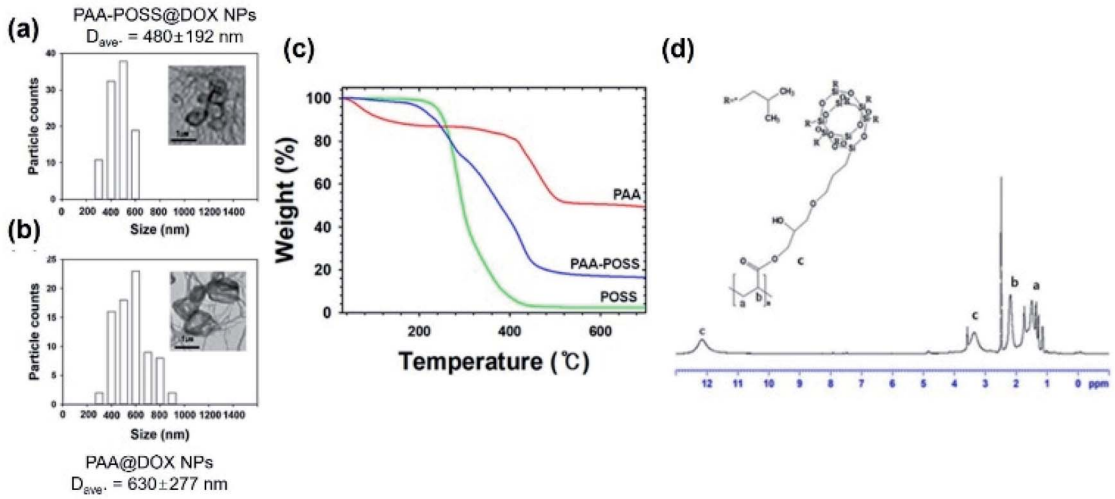

Fig. 3 The particle size distribution and TEM image of (a) PAA-POSS@DOX NPs and (b) PAA@DOX NPs; the TGA spectra (c) of POSS (green line), PAA-POSS (blue line), and PAA (red line); and (d) the ^{1}H-NMR spectra of POSS-PAA.

Smaller size, more uniform distribution, less aggregation, and better dispersion can be seen in PAA-POSS@DOX compared with PAA@DOX. This appears to be due to the more stable fixation of the drug in the strongly hydrophobic POSS and POSS, helping the uniform formation of particles.[25,26]

The TGA data of PAA, POSS and PAA-POSS@DOX are shown in Fig. 3(b). The thermal degradation of PAA shows an approximately 13% weight decrease up to 415 °C, then a second degradation starts to result in 49% char yield. Thermal degradation of POSS starts at 200 °C then almost fully sublimes to leave less than 2% char. The thermal degradation of PAA-POSS starts at 200 °C, similar to POSS, but the char yield is 16%. The thermal degradation of PAA-POSS shows both the behavior of POSS and the PAA main component, but the char yield is lower than that of PAA.

The doxorubicin entrapment efficiency (EE) of the synthesized PAA-POSS@DOX is 75.0%, much higher than the 49.1% of PAA@DOX, which appears to be due to the highly hydrophobic nature of POSS strongly capturing the drug, resulting in a high loading efficiency. The release of the drug with time at different pH values for PAA@DOX and PAA-POSS@DOX is shown in Fig. 4(a). There was no difference in the amount of release of the drug at pH 7.4 with time between PAA@DOX and PAA-POSS@DOX, but at pH 5.0 the cumulative release of the drug after 6 h to 24 h was around 80% for PAA-POSS@DOX compared with 40% for PAA@DOX, which is a big difference in the drug release (about twice the value). This appears to be due to POSS allowing PAA to react faster to the pH of the surroundings. This is similar to the effect of POSS observed in a previous experiment.

SI4 shows that the absolute ζ-potential values of PAA-POSS@DOX particles are about 20 mV more in the range of pH 4 to pH 8. This result considered that PAA-POSS@DOX particles are present in a very stable colloidal dispersion over almost all pH ranges. It can also be confirmed that when the pH changes from 7 to a weakly acidic (pH 5) environment due to the drug release mechanism, the PAA-POSS@DOX ζ-potential has a stronger anionization from −21.7 mV to −24.6 mV. This indicates that when the pH is lowered, the anionic carboxylic acid groups of PAA-POSS tend to rapidly dissolve the PAA chains. At this time, the ζ-potential values also decrease, which proved that the PAA-POSS@DOX nanoparticles have very good dispersibility and that drug release is possible. PAA-POSS@DOX could be used as a pH-sensitive drug carrier in the design of anticancer drugs.

Fig. 4(B) shows the effect of repetitive change in the pH of PBS from 7.4 to 5.0 on drug release. The first 6 h release at pH 7.4 was only ∼10%, but when the pH was changed to 5.0, fast release was observed with a cumulative release at 12 h of ∼65%. When the pH was changed back to 7.0, the behavior is similar to the first. In the second pH 5 stage from 18 h onwards, there was no further release as the maximum release had already occurred. These results suggest that PAA-POSS@DOX has the possibility of being a targeted on/off drug delivery system reacting specifically and quickly to the surrounding pH.

Breast cancer cells were treated with different concentrations of PAA@DOX, PAA-POSS@DOX, and free DOX for different periods, and the self-death effect of the cancer cells was evaluated. The different concentrations were 0, 5, 10, 20, and 40 μg ml^{-1}, and the self-death effect was evaluated after 24 and 48 h, as shown in Fig. 5 (A) and (B). As can be seen in Fig. 5(A), PAA-POSS@DOX induced a greater self-death effect in MDA-MB-231 cancer cells after 24 h at all concentrations compared with that of PAA@DOX. In the case of free DOX, it is reported that due to its toxicity, its injection into the body induces high oxidative stress and brings about side effects such as acute cardiotoxicity, a decrease in white blood cells, nausea, and loss of hearing.[27–30] As can be confirmed from the data, free DOX exhibits the highest self-death effect. The self-death effect after 48 h shows no difference between PAA-POSS@DOX and PAA@DOX. This

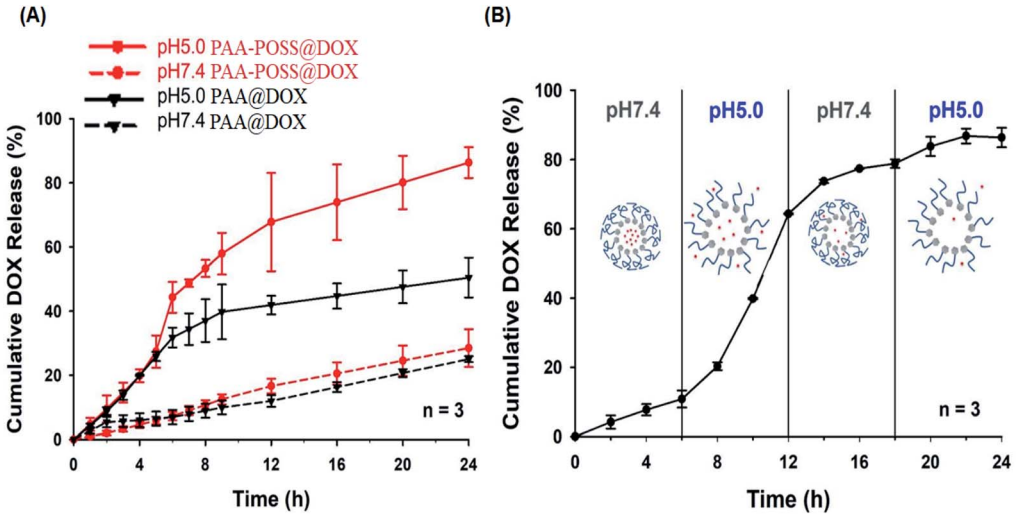

Fig. 4 *In vitro* pH-responsive release of DOX from (A) PAA-POSS@DOX NPs (red) and PAA@DOX NPs (black) for 24 h in pH 5.0 and pH 7.4 PBA buffer solution, 37.5 °C and (B) extended drug release profiles of PAA-POSS@DOX NPs by changing the release medium to PBS (pH 7.4 and 5.0) for 24 h.

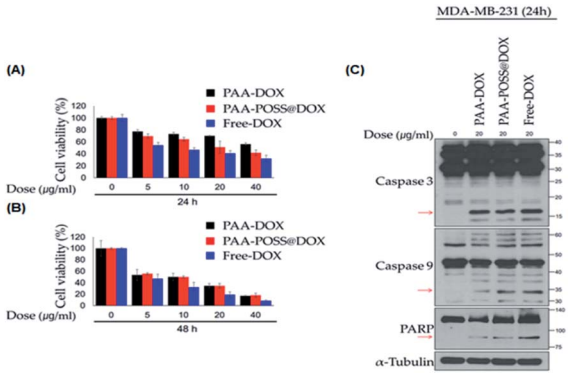

Fig. 5 (A) and (B) MDA-MB-231 cells were treated with various concentrations of PAA@DOX, PAA-POSS@DOX and free DOX for 24 h and 48 h. Cell viability was measured by the MTT assay. (C) MDA-MB-231 cells were treated with 20 μg ml^{-1} of PAA@DOX, PAA-POSS@DOX and free DOX for 24 h. Cell lysates were analyzed by immunoblotting.

appears to be due to the acceleration of the drug release at the target area due to the introduction of POSS, resulting in depletion or only a minute amount of DOX at around 48 h. In the confirmation of the death signal in the cell, the cleaved caspase 3 and caspase 9 PARP shown in Fig. 5(C) show similar cell death at concentrations above 20 μg ml^{-1} as when using free DOX. The cell death of MDA-MB-231 cancer cells after 24 and 48 h when concentrations of over 20 μg ml^{-1} are used is evident in Fig. S2.†

Experimental

Materials

PSS-(2,3-propanediol)propoxy-heptaisobutyl substituted (POSS), poly(acrylic acid) (PAA, M_w: 5000 g mol^{-1} partial sodium), doxorubicin hydrochloride (DOX), tetrahydrofuran (THF), and sulfuric acid (95.0%) were obtained from Sigma Aldrich (Seoul, Korea) and used as received. Human metastatic breast cancer cell line MDA-MB-231 was purchased from Korean Cell Line Bank (KCLB). All other chemicals were of analytical grade.

Synthesis of PAA-POSS

To prepare PAA-POSS, 10 g PAA, 95 mg POSS and 56 μl sulfuric acid was dissolved in 50 ml THF in a 3-neck reactor and stirred under reflux at 100 °C for 5 h with a mechanical stirrer. In order to remove POSS that did not participate in the synthesis, the synthesized POSS-PAA was filtered with chloroform using a vacuum pump. The filtered compound was dried in a vacuum oven at 150 °C for 30 minutes to obtain a white powder.

Preparation of PAA-POSS@DOX

For the fabrication of PAA-POSS loaded DOX, 3 mg PAA-POSS and 1 mg DOX were dissolved in 10 ml of distilled water/DMF (1 : 1 v/v) mixture and then sonicated for 1 h under ice water condition. After sonication, PAA-POSS@DOX is stirred for 1 h at room temperature. DOX encapsulation was carried out on the basis of self assembly process. The mixture was poured into dialysis tubing (spectra/Por®, 3.5 kD cut-off) and dialyzed against distilled water at room temperature under magnetic stirring for 6 h. Afterwards, the distilled water was exchanged every hour in order to remove the THF residues.

In vitro drug release experiments and drug loading efficiency

In vitro DOX release experiments were carried out. 5 ml PAA-DOX and POSS-graft-PAA-DOX solution was placed in a dialysis tube of MWCO 3.5 kD and stabilized at room temperature. The dialysis bag was submerged in pH 5.0 and 7.4 PBS (50 ml), and incubated at 37 °C for 24 h. The released doxorubicin in the incubation buffer was collected at pre-determined intervals and was frozen for further quantitative detection using a refractive index detector and analysis. Quantitative analysis was performed by measuring the absorbance at 480 nm on a UV-Visible spectrophotometer to calculate the amount of DOX, and the cumulative release of DOX (%) was calculated with the following equation.

$$\text{Cumulative release of DOX } (\%) = \frac{v_C \sum_{1}^{n-1} C_i + v_0 C_n}{m_0} \times 100\% \quad (1)$$

And the following equation was used to calculate the drug loading efficiency.

$$\text{Drug loading efficiency} = \frac{\text{amount of drug in nanoparticles}}{\text{amount of drug initially added}} \times 100 \quad (2)$$

$$\text{Drug loading contents} = \frac{\text{amount of drug}}{\text{amount of drug and polymer}} \times 100 \quad (3)$$

In vitro cell assay

An MTT assay was carried out by inoculating the cells in a 96-well culture plate and then incubating them in the culture medium until 80% merging. The MDA-MB-231 cells were treated with different concentrations of samples for 24 h and then incubated for 2 h with MTT reagent. The blue formazan crystals were dissolved in DMSO and the formazan level was measured using an Infinite M200 PRO plate reader (Tecan Group Ltd., Männedorf, Switzerland) at 570 nm. To carry out immunoblotting analysis, the cells were washed with cold PBS and then dissolved in Triton dissolved buffer solution containing protease- and phosphatase-inhibiting agents. After 30 min incubation over ice, the dissolved sample was centrifuged for 10 min at 4 °C, 13 000 rpm, and the supernatant was collected. The dissolved material in the supernatant was resolved with an 8–15% SDS-polyacrylamide gel, then transferred to a nitrocellulose membrane (GE Healthcare Life Sciences, Chicago, Illinois). The membrane was blocked in 5% skim milk for 1 h, then incubated overnight with the primary antibody. The membrane was incubated with a secondary

antibody modified with horseradish peroxidase (HRP) for 1 h, then detected with an ECL western blotting kit (Biomax Co., Ltd, Seoul, Korea).

Characterization

FTIR analysis was carried out on PerkinElmer Spectrum II with KBr pellets. ^{1}H-NMR analysis was carried out on a JEOL 400. $CDCl_3$ was used as the ^{1}H-NMR solvent. X-ray photoelectron spectroscopy (XPS) was carried out on a Nexsa using microfocus monochromatic Al-Kα at 1486.6 eV, with an energy resolution (Ag $3d_{5/2}$) of $\leq$0.5 eV, sensitivity of 4 000 000 cps, ultimate vacuum of $<5.0 \times 10^{-9}$ mbar, and X-ray spot size of 10–400 μm. The analyzer was a double-focusing, hemispherical analyzer with a 128-channel detector and the depth profiling was carried out with a MAGCIS dual mode ion source. Analysis of the thermal stability was carried out on a TGA N-1000 from 25 to 700 °C. FE-TEM analysis was carried out on a JEM-2100F.

Conclusions

To develop an organic/inorganic hybrid drug delivery system that can react to minute changes in the pH of the environment, such as that in the cancer microenvironment, POSS was introduced to PAA. The loading efficiency of 480 $\pm$ 192 nm PAA-POSS nanoparticles loaded with doxorubicin (anti-cancer drug) is over 75%, and they reacted sensitively to weakly acidic conditions to quickly release the drug at the targeted area. The possibility of developing a targeted drug delivery system that kills MDA-MB-231 cancer cell lines has been confirmed.

Conflicts of interest

There are no conflicts to declare.

Acknowledgements

This work was supported by a National Research Foundation of Korea (NRF) grant funded by the Korean government (No. R-2018-00235) the National Research Foundation of Korea (NRF) funded by the Korea government (NRF-2018R1A5A2025964 and NRF-2022R1A2C1011914), as well as by the Technology Innovation Program (nano product performance safety evaluation technology development and business support project) (20014731, development of safety evaluation method for nonwoven and garment products containing nanofiber) funded by the Ministry of Trade, Industry & Energy (MOTIE, Korea).

Notes and references

1 Y. Pu, L. Zhang, H. Zheng, B. He, *et al.* Drug release of pH-sensitive poly (L-aspartate)-b-poly (ethylene glycol) micelles with POSS cores, *Polym. Chem.*, 2014, **5**(2), 463–470.
2 Y. Pu, S. Chang, H. Yuan, *et al.* The anti-tumor efficiency of poly (L-glutamic acid) dendrimers with polyhedral oligomeric silsesquioxane cores, *Biomaterials*, 2013, **34**(14), 3658–3666.
3 T. L. Kaneshiro, X. Wang and Z. R. Lu, Synthesis, characterization, and gene delivery of poly-L-lysine octa (3-aminopropyl) silsesquioxane dendrimers: nanoglobular drug carriers with precisely defined molecular architectures, *Mol. Pharm.*, 2007, **4**(5), 759–768.
4 X. J. Loh, Z. X. Zhang, K. Y. Mya, *et al.* Efficient gene delivery with paclitaxel-loaded DNA-hybrid polyplexes based on cationic polyhedral oligomeric silsesquioxanes, *J. Mater. Chem.*, 2010, **20**(47), 10634–10642.
5 H. Ghanbari, B. G. Cousins and A. M. Seifalian, A nanocage for nanomedicine: polyhedral oligomeric silsesquioxane (POSS), *Macromol. Rapid Commun.*, 2011, **32**(14), 1032–1046.
6 C. McCusker, J. B. Carroll and V. M. Rotello, Cationic polyhedral oligomeric silsesquioxane (POSS) units as carriers for drug delivery processes, *Chem. Commun.*, 2005, (8), 996–998.
7 A. Almutary and B. Sanderson, Toxicity of four novel Polyhedral Oligomeric Silsesquioxane (POSS) particles used in anti-cancer drug delivery, *J. Appl. Pharm. Sci.*, 2017, **7**, 101–105.
8 K. O. Kim, Y. A. Seo, B. S. Kim, *et al.* Transition behaviors and hybrid nanofibers of poly(vinyl alcohol) and polyethylene glycol–POSS telechelic blends, *Colloid Polym. Sci.*, 2011, **289**, 863–870.
9 K. O. Kim and I. S. Kim, Cytocompatibility and osteogenesis of adipose tissue-derived stem cells on POSS-PEG coated collagen, *J. Nanosci. Nanotechnol.*, 2018, **18**, 4439–4444.
10 M. Stubbs, P. M. McSheehy, J. R. Griffiths, *et al.* Causes and consequences of tumour acidity and implications for treatment, *Mol. Med. Today*, 2000, **6**(1), 15–19.
11 R. Van Sluis, Z. M. Bhujwalla, N. Raghunand, *et al.* In vivo imaging of extracellular pH using 1H MRSI, *Magn. Reson. Med.*, 1999, **41**(4), 743–750.
12 D. B. Leeper, K. Engin, A. J. Thistlethwaite, *et al.* Human tumor extracellular pH as a function of blood glucose concentration, *Int. J. Radiat. Oncol., Biol., Phys.*, 1994, **28**(4), 935–943.
13 X. Hu, R. Wang, J. Yue, *et al.* Targeting and anti-tumor effect of folic acid-labeled polymer–doxorubicin conjugates with pH-sensitive hydrazone linker, *J. Mater. Chem.*, 2012, **22**(26), 13303–13310.
14 M. Li, Z. Tang, H. Sun, *et al.* pH and reduction dual-responsive nanogel cross-linked by quaternization reaction for enhanced cellular internalization and intracellular drug delivery, *Polym. Chem.*, 2013, **4**(4), 1199–1207.
15 H. Wang, F. Xu, D. Li, *et al.* Bioinspired phospholipid polymer prodrug as a pH-responsive drug delivery system for cancer therapy, *Polym. Chem.*, 2013, **4**(6), 2004–2010.
16 X. Zhang, Y. Lin and R. J. Gillies, Tumor pH and its measurement, *J. Nucl. Med.*, 2010, **51**(8), 1167–1170.
17 K. Engin, D. B. Leeper, J. R. Cater, *et al.* Extracellular pH distribution in human tumours, *Int. J. Hyperthermia*, 1995, **11**(2), 211–216.
18 T. Volk, E. Jähde, H. P. Fortmeyer, K. H. Glüsenkamp, *et al.* pH in human tumour xenografts: effect of intravenous administration of glucose, *Br. J. Cancer*, 1993, **68**(3), 492–500.

19 A. S. Ojugo, P. M. McSheehy, D. J. McIntyre, *et al.* Measurement of the extracellular pH of solid tumours in mice by magnetic resonance spectroscopy: a comparison of exogenous 19F and 31P probes, *NMR Biomed.*, 1999, **12**(8), 495–504.

20 E. S. G. Choo, B. Yu and J. Xue, Synthesis of poly (acrylic acid)(PAA) modified Pluronic P123 copolymers for pH-stimulated release of doxorubicin, *J. Colloid Interface Sci.*, 2011, **358**(2), 462–470.

21 Y. Dai, C. Zhang, Z. Cheng, *et al.* pH-responsive drug delivery system based on luminescent CaF2: Ce3+/Tb3+-poly (acrylic acid) hybrid microspheres, *Biomaterials*, 2012, **33**(8), 2583–2592.

22 B. Tian, S. Liu, S. Wu, *et al.* pH-responsive poly (acrylic acid)-gated mesoporous silica and its application in oral colon targeted drug delivery for doxorubicin, *Colloids Surf., B*, 2017, **154**, 287–296.

23 G. Li, S. E. N. Song, L. E. I. Guo, *et al.* Self-assembly of thermo-and pH-responsive poly (acrylic acid)-b-poly (N-isopropylacrylamide) micelles for drug delivery, *J. Polym. Sci., Part A: Polym. Chem.*, 2008, **46**(15), 5028–5035.

24 F. K. Wang, X. Lu and C. He, Some recent developments of polyhedral oligomeric silsesquioxane (POSS)-based polymeric materials, *J. Mater. Chem.*, 2011, **21**(9), 2775–2782.

25 K. O. Kim, B. S. Kim and I. S. Kim, Self-assembled core-shell poly (Ethylene Glycol)-POSS nanocarriers for drug delivery, *J. Biomater. Nanobiotechnol.*, 2011, **2**(3), 201.

26 K. Rozga-Wijas and M. Sierant, Daunorubicin-silsesquioxane conjugates (POSS-DAU) for theranostic drug delivery system: Characterization, biocompatibility and drug release study, *React. Funct. Polym.*, 2019, **143**, 104332.

27 R. Injac and B. Strukelj, Recent advances in protection against doxorubicin-induced toxicity, *Technol. Cancer Res. Treat.*, 2008, **7**(6), 497–516.

28 G. Takemura and H. Fujiwara, Doxorubicin-induced cardiomyopathy: from the cardiotoxic mechanisms to management, *Prog. Cardiovasc. Dis.*, 2007, **49**(5), 330–352.

29 Y. QuanJun, Y. GenJin, W. LiLi, *et al.* Protective effects of dexrazoxane against doxorubicin-induced cardiotoxicity: a metabolomic study, *PLoS One*, 2007, **12**(1), e0169567.

30 C. Carvalho, R. X. Santos, S. Cardoso, *et al.* Doxorubicin: the good, the bad and the ugly effect, *Curr. Med. Chem.*, 2009, **16**(25), 3267–3285.